

## TRANSETHOSOMES AS BREAKTHROUGH TOOL FOR CONTROLLED TRANSDERMAL DELIVERY OF DEXKETOPROFEN TROMETAMOL: DESIGN, FABRICATION, STATISTICAL OPTIMIZATION, *IN VITRO*, AND *EX VIVO* CHARACTERIZATION

SARA M. SOLIMAN<sup>1</sup> , KAREEM OMAR RASHWAN<sup>1</sup>, MAHMOUD TEAIMA<sup>2</sup> , BHASKARA R. JASTI<sup>3</sup>, MOHAMED AHMED EL-NABARAWI<sup>2</sup> , KHALED M. ABDEL-HALEEM<sup>1\*</sup> 

<sup>1</sup>Department of Pharmaceutics and Industrial Pharmacy, Faculty of Pharmacy, October 6 University, 6<sup>th</sup> of October City, Giza, <sup>2</sup>Department of Pharmaceutics and Industrial Pharmacy, Faculty of Pharmacy, Cairo University, Cairo, Egypt, <sup>3</sup>Department of Pharmaceutics and Medicinal Chemistry, Thomas J. Long School of Pharmacy and Health Sciences, University of the Pacific, Stockton, USA  
Email: khaled.mohamed.pha@o6u.edu.eg

Received: 02 Jul 2022, Revised and Accepted: 10 Aug 2022

### ABSTRACT

**Objective:** Transethosomes (TEs) have introduced an emerging avenue of interest in vesicular research for transdermal delivery of drugs and can be a proper delivery system for painkillers like NSAIDs. This study aimed to formulate and characterize the potential of TE to enhance the transdermal transport of Dexketoprofen trometamol (DKT) to achieve controlled pain management compared to DKT solution.

**Methods:** Factorial design (2<sup>3</sup>) was adopted to appraise the influence of independent variables, namely, Lipoid S100 and surfactant concentrations and surfactant type (X<sub>3</sub>) on the % solubilization efficiency (% SE), vesicle size (VS), and % release efficiency (% RE). Thin film hydration was the preferred approach for preparing TEs where vesicle size, zeta potential, polydispersity index, %SE and %RE were investigated. The optimized formula was nominated and subjected to several studies. For the permeation study, optimum TE was incorporated into carbapol gel base for comparison with DKT solution. Also, an accelerated stability study was assessed for optimized formula.

**Results:** All the prepared DKT-loaded TEs revealed acceptable VS, PDI, and ZP. The highest %SE (86.08±1.05 %) and lowest %RE (44.62±1.36 %) were observed in case of F1. The optimized formula (F1) displayed VS of 133.2±1.62 nm, PDI of 0.342±0.03 and ZP of -21.6±2.45 mV. F1 revealed enhanced skin permeation of a 2.6-fold increase compared with DKT solution. Moreover, F1 was stable upon storage and a non-significant change (P>0.05) was observed.

**Conclusion:** DKT was successfully incorporated into vesicle carrier and can signify an alternative option for providing this therapy, bypassing the poor bioavailability and considerable adverse consequences of using the oral route besides improved patient compliance.

**Keywords:** Transethosomes, Transdermal drug delivery, Dexketoprofen trometamol, Permeation

© 2022 The Authors. Published by Innovare Academic Sciences Pvt Ltd. This is an open access article under the CC BY license (<https://creativecommons.org/licenses/by/4.0/>)  
DOI: <https://dx.doi.org/10.22159/ijap.2022v14i6.45726>. Journal homepage: <https://innovareacademics.in/journals/index.php/ijap>

### INTRODUCTION

Since the skin is by far the most complicated organ in the human body, it tends to provide a challenge to the nanomedicines field as it affords respective merits over other administration routes including escaping of first-pass effect, minimal changes in plasma drug levels and respectable patient compliance [1]. Due to the obvious complex skin aspects, transdermal administration stands as a challenging task for the therapeutic agent to exhibit its therapeutic activity. The Stratum corneum (SC) represents the epidermis's top layer, and acts as a barricade to drug penetration [2]. Drugs that possess either low or high partition coefficient face struggle in reaching systemic circulation and therefore this can be resolved via the use of innovative drug delivery vesicles such as ultra-deformable vesicle [3, 4].

Dexketoprofen trometamol (DKT) is an NSAID that was developed as a water-soluble trometamine that acts as a painkiller and anti-inflammatory in case of musculoskeletal disorders associated with pain such as back pain and osteoarthritis [5]. It is generally established that traditional routes of administration have several issues, as mentioned before and these challenges can be resolved by inventing a transdermal drug delivery (TDD) *via* use of special nanocarriers as vesicles [6].

Vesicular systems appear to represent a new era of research in the nano-delivery field owing to their physicochemical properties, such as deformability, size, and charge [7]. Transethosomes (TEs) seems like one of those critical vesicular systems which were originally envisioned by Song *et al.* [4]. The TE system includes the essential components of conventional ethosomes as well as surfactant (SAA) in their composition [8]. The presence of a high concentration of ethanol in TEs fluidizes the stratum corneum's lipid layer and enables them to infiltrate *via* microscopic holes generated by fluidization [9]. The inclusion of SAA provides the produced vesicles

flexibility, where they can deform and pass *via* the skin-tight constriction with no observable loss [1, 10]. Additionally, TEs offer a semisolid dosage form for administration, which encourages good compliance besides improved drug permeation *via* skin and evades pre-systemic absorption [4, 11]. Subsequently, TE represents a suitable nanocarrier for transdermal delivery of DKT. Different techniques of DKT delivery have been studied, notably to produce oral formulations [5]. Nevertheless, there has been limited study on dermal or local DKT delivery [12]. Accordingly, this study intended to formulate and characterize the potential of TE to enhance the transdermal transport of DKT to achieve an efficient anti-inflammatory and pain management compared to DKT solution.

### MATERIALS AND METHODS

#### Materials

Dexketoprofen trometamol (gift sample from Marcyrl Pharmaceutical Industries, Obour, Egypt); Lipoid S100 and Cremophor RH 40 (Sigma-Aldrich, Co., Steinheim, Germany); Labrafil (Gattefosse, Saint-Priest Cedex, France); potassium dihydrogen phosphate, disodium hydrogen phosphate (EL Nasr chemical company, Cairo, Egypt); Carbopol 940®; triethanolamine (Nouresh' shark Company, Cairo, Egypt); methanol-HPLC grade (Sigma-Aldrich, MO, USA); Deionized Water for Injection (Al Mottahedoon Pharma, Cairo, Egypt); Dialysis cellophane membrane (1-inch width-cut off 12000-15000 Da, HIMEDIA, India)

#### Methods

##### Construction of the experimental design

DKT-loaded TE was created and optimized utilizing the findings of 2<sup>3</sup> full factorial designs employing Design Expert® software version 7. (Stat-Ease, Inc., Minneapolis, MN, USA). The experimental design

entails investigating the impact of three independent variables, viz., X<sub>1</sub>: Lipoid S100 concentration, X<sub>2</sub>: SAA concentration, and X<sub>3</sub>: SAA type on DKT TE solubilization efficiency (Y<sub>1</sub>, %SE), mean vesicle size

(Y<sub>2</sub>, VS) and percentage release efficiency (Y<sub>3</sub>, %RE). Eight sets were constructed based on the findings of the preceding stated design, with all the variables and levels presented in (table 1).

**Table 1: 2<sup>3</sup> Factorial design DKT loaded TEs fabrication and optimization**

Independent variables	Levels	
	Low	High
X <sub>1</sub> : Lipoid S100 concentration	1%	4%
X <sub>2</sub> : SAA concentration	0.2%	0.8%
X <sub>3</sub> : SAA type	Labrafil	Cremophor RH 40
Dependent variables	Desirability constraints	
Y <sub>1</sub> : SE (%)	Maximize	
Y <sub>2</sub> : VS (nm)	In-range	
Y <sub>3</sub> : RE (%)	Minimize	

### Formulation of DKT-loaded TEs

The drug was enclosed in lipid vesicles by using a thin film hydration process. Firstly, the quantified weight of Lipoid S100 and SAA (Labrafil and Cremophore RH 40) with DKT according to the composition shown in (table 2) were transferred in a clean, dry round bottom flask where methanol was utilized to dissolve the lipid components. To establish a thin lipid layer just above the lipid transition temperature, a rotary evaporator was utilized. It is kept under pressure for 24 h to remove organic solvent residues. By spinning at 60 revolutions per min, the formed film was hydrated with DKT (1% w/v) ethanolic 20% v/v solution. Sonication is utilized to shrink the vesicles to a more controllable size [13, 14].

### Characterization of the prepared DKT-loaded TEs

#### Calculation of DKT percentage solubilization efficiency (%SE)

The solubilization efficiency of DKT-loaded TEs was determined *via* the ultracentrifugation method. TEs were separated using a cooling centrifuge at 15,000 rpm and 4 °C for 60 min. The sediment and supernatant liquid was separated, and the amount of drug in the sediment was assessed by rupturing the vesicles with methanol, while the amount of DKT was quantified spectrophotometrically at max 260 nm [1, 15]. SE can be calculated as follows:

$$\%SE = \frac{\text{Amount of encapsulated DKT}}{\text{Initial amount of DKT}} * 100$$

#### Vesicle size (VS), polydispersity index (PDI), and zeta potential (ZP) determination of the DKT-loaded TEs

Sample dilutions were adopted followed by analysis at room temperature using Malvern Zetasizer [1, 7, 16, 17].

#### *In vitro* release studies of DKT-loaded TEs

*In vitro* DKT release from TEs was carried out using the dialysis bag method as reported by Verma *et al.* [18]. In this method, 1 ml of TEs suspension was loaded to dialysis membrane (previously soaked in phosphate buffer saline PBS, pH = 7.4) followed by immersion of soaked dialysis bag containing TEs suspension in release medium of 500 ml PBS where the DKT release was proceeded using USP dissolution system, Distek Type II at 37±0.5 °C and 100 rpm. At varying time intervals, samples were gathered and replaced immediately with 1 ml PBS held at the same temperature. The samples were investigated at the predefined max λ<sub>max</sub> = 260 nm using a UV spectrophotometer [19].

#### Selection of the optimized formula

Optimization of DKT-loaded TEs formulae was implemented based on the prediction of desirability value. The metrics used to pick out the optimum formula was accomplishing VS in range <250 nm, lowest %RE besides achieving the highest % SE.

#### Incorporation of DKT-loaded TEs into gel

DKT-loaded TEs gel was prepared by gently swirling the optimized DKT-loaded TEs into a pre-prepared gel base. Carbopol 940® (1 % w/w) was soaked in distilled water and left to thicken inside the

refrigerator overnight to create the gel base. After that, gel formation necessitates neutralization, which was accomplished by adding triethanolamine dropwise alongside constant agitation until a pH of 7.0 was achieved, resulting in the formation of a unified translucent gel [20, 21].

#### Characterization of the DKT-loaded TE gels

##### Vesicles morphology of the optimized DKT loaded TEs using a Transmission electron microscope (TEM)

The vesicular dispersion was deposited on a carbon-coated copper grid, dyed with 1.5 % (w/v) phosphotungstic acid, and then photographed and inspected for morphological evaluation [22].

##### Fourier transform infrared spectroscopy (FT-IR)

Potassium bromide (KBR) pellet technique was adopted to perform FT-IR analysis of pure DKT and the optimal formula where a mixture of sample and KBr was pulverized at 10 kg/cm in a hydraulic press, yielding a translucent pellet which inserted in the sample container and scanned in FT-IR from 4000 cm<sup>-1</sup> to 500 cm<sup>-1</sup> [23-25].

##### *Ex-vivo* skin permeation evaluation of DKT-loaded TEs gel

The transdermal permeability of DKT loaded TEs gel and DKT solution through male *Wistar* rat (150-170 g) skin was studied (purchased from the animal house of Applied Research Center for Medicinal Plant, Egypt and the study was approved by the Institutional Animal Ethics Committee, Faculty of Pharmacy, Cairo University, Egypt, code PI 2332). Rats were kept in cages at 27±2 °C with an alternate 12 h light and dark cycle and unrestricted access to food and drink. The hair on the rat's dorsal side was gently excluded with an electrical razor. Excision of the shaved skin part (full thickness) was carefully done, and the subcutaneous fat tissue was removed. Following that, skin that has been removed was properly rinsed with phosphate buffer saline (PBS, pH =7.4), and before being carved into parts, it is thoroughly checked for integrity as well as any fractures or furrows which were then used for permeation studies using Franz diffusion apparatus with a diffusion surface area of 1.7 cm<sup>2</sup> and the SC facing the donor compartment [22, 26]. The test was set up analogous to the *in vitro* release, except the membrane was replaced by dorsal skin, with the SC facing the donor compartment. To maintain sink conditions, specimens were drained on a constant schedule and restored with an equal volume of fresh medium. Each sample was analyzed using HPLC at λ<sub>max</sub> of 260 nm.

##### Stability Study of the optimized DKT-loaded TEs gel

The stability studies of the optimized DKT-loaded TEs gel include assessment of VS, PDI, ZP, %EE, and %RE using the same methodology after three months of storage in sealed glass vials at 5±3 °C.

## RESULTS AND DISCUSSION

### Characterization of the prepared DKT-loaded TEs

#### Influence of formulation variables on solubilization efficiency

Still, the drug encapsulation within the lipid vesicle is the challenge for the invention of nanocarrier that affords better stability

formulation, required delivery, and permeability [27]. The outcomes for %SE of different prepared TEs are revealed in (table 2) where the value ranged from 22.54±1.12% to 86.08±1.05% where the TEs comprising the high concentration of Lipoid S100 and labrafil as SAA with low concentration recorded the uppermost %SE compared to other prepared DKT loaded TEs as displayed in (fig 1). As well, the regression analysis presented that formulation variables had a significant impact ( $p < 0.0001$ ) on %SE as revealed in (table 3). Based on the sign of coefficient estimate for the influence of Lipoid S100 concentration, SAA concentration, and SAA type (+8.91,-12.49 and -10.78 respectively), the %SE of TEs were found to have a positive correlation with the former and negatively with the latter. Additionally, it was established that the SAA concentration ( $X_2$ ) signifies the most influential variable on TE %SE, as illustrated by the sum of their square values (1269.41 for  $X_1$ , 2495.50 for  $X_2$  and 1858.04 for  $X_3$ ) and f-value (650.59 for  $X_1$ , 1279.25 for  $X_2$  and 952.47 for  $X_3$ ). According to (fig. 1), the %SE of the formed DKT-loaded TEs was proportional to the Lipoid S100 concentration, with a noticeable rise in %SE as the Lipoid S100 concentration increased from low (1%) (59.7±1.21%) to high level (4%) (86.08±1.05%). That could be because phospholipid forms a more condensed and packed structure, contributing to increased drug entrapment in this lipidic area [28]. Moreover, boosting the concentration of Lipoid S100 resulted in the formation of a large number of TE vesicles which hence increases the dimensions of the domain and makes space for

the entrapment of the drug [29]. Concerning the impact of  $X_2$  on %SE where other factors are constant, altering SAA concentration from 0.2% to 0.8% cause a significant decrease in %SE of DKT loaded TE from 86.08±1.05% (0.2% SAA) to 59.70±1.21% (0.8% SAA) and this is confirmed by the negative sign of the coefficient of estimates (-12.49). It was reported that increasing concentration of SAA or edge activator causes a reduction in vesicular size and hence causes a decrease in %SE [30]. As well, the decrease in %SE with a high level of SAA concentration (Labrafil or Cremophore) may be indicative of the presence of micelle structure in conjunction with vesicles in the formulation; micelles tend to have a lower entrapment capability over vesicles [28]. Concerning SAA type ( $X_3$ ) where other factors are constant, it was observed that upon shifting the SAA type from Labrafil (F1) to cremophore (F5), a significant decrease in %SE of DKT loaded TEs from 86.08±1.05% to 70.88±0.09% and similarly it was confirmed by the negative sign for the coefficient of estimates (-10.78). This is consistent with the findings of Aboud *et al.* [31] and would be confirmed based on SAA hydrophilic-lipophilic balance (HLB) values; labrafil and cremophore, which was 9 for the former and 15 for the latter. Low HLB SAAs are known to be more lipophilic, which promotes drug entrapment [32].

The coded equation that clarified the influence of  $X_1$ ,  $X_2$  and  $X_3$  on %SE is as follows:

$$Y_1 = 52.04 + 8.91 X_1 - 12.49 X_2 - 10.78 X_3$$

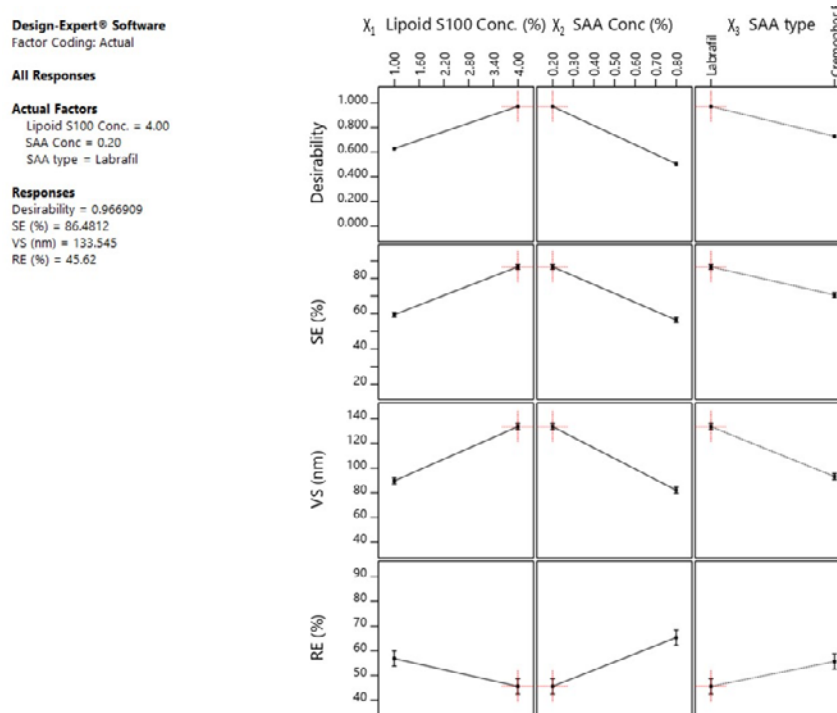


Fig. 1: Independent formulation variables effect ( $X_1$ : Lipoid S100;  $X_2$ : SAA conc. and  $X_3$ : SAA type) on solubilization efficiency (%SE), vesicle size (VS), and release efficiency (%RE) beside the overall desirability (results were expressed as mean±SD, n=3)

Table 2: The 2<sup>3</sup> factorial experimental design of DKT-loaded TEs included experimental runs, independent variables, and reported outcomes

Formulae code	Independent variables			Responses				
	$X_1$ Lipoid S100 conc (%)	$X_2$ SAA conc (%)	$X_3$ SAA type	PDI	ZP (mV)	$Y_1$ SE (%)	$Y_2$ VS (nm)	$Y_3$ RE (%)
F1	4%	0.20%	Labrafil	0.342±0.03	-21.6±2.45	86.08±1.05	133.2±1.62	44.62±1.36
F2	1%	0.20%		0.466±0.05	-27.5±1.75	59.7±1.21	89.97±2.11	57.92±2.21
F3	4%	0.80%		0.179±0.24	-19.6±2.47	56.65±0.08	82.49±0.60	66.39±1.24
F4	1%	0.80%		0.300±0.06	-24.4±0.45	48.84±1.28	68.55±0.57	73.71±1.58
F5	4%	0.20%	Cremophor	0.221±0.05	-20.50±1.25	70.88±0.09	93.51±1.78	56.72±2.38
F6	1%	0.20%		0.343±0.23	-19.00±1.50	41.46±1.13	60.21±0.78	65.3±3.12
F7	4%	0.80%		0.133±0.09	-20.3±2.33	30.18±0.86	51.61±2.50	72.38±1.87
F8	1%	0.80%		0.265±0.32	-26.21±1.54	22.54±1.12	50.36±3.03	82.98±2.6

Data represented as a mean±SD; n=3, PDI: Polydispersity index; ZP: Zeta potential; SE: Solubilization efficiency; VS: Vesicle size; RE: Release efficiency

Table 3: Analysis of variance of DKT loaded TEs responses

Source	Coefficient estimates	Sum of squares	Mean square	F-value	*p-value	
%SE (Y <sub>1</sub> )						
Model	-	5622.68	1020.86	523.32	<0.0001	Significant
X <sub>1</sub>	8.91	1269.14	1269.14	650.59	<0.0001	
X <sub>2</sub>	-12.49	2495.50	2495.50	1279.25	<0.0001	
X <sub>3</sub>	-10.78	1858.04	1858.04	952.47	<0.0001	
VS (Y <sub>2</sub> )						
Model	-	9451.45	1770.64	285.37	<0.0001	Significant
X <sub>1</sub>	11.47	2103.14	2103.14	338.96	<0.0001	
X <sub>2</sub>	-15.48	3836.56	3836.56	618.33	<0.0001	
X <sub>3</sub>	-14.81	3511.75	3511.75	565.98	<0.0001	
%RE (Y <sub>3</sub> )						
Model	-	1954.43	327.22	33.15		
X <sub>1</sub>	-4.97	396.01	396.01	40.12	0.0001	Significant
X <sub>2</sub>	8.86	1256.70	1256.70	127.30	<0.0001	
X <sub>3</sub>	4.34	301.72	301.72	30.56	0.0004	

X<sub>1</sub>: lipid S100 concentration; X<sub>2</sub>: SAA concentration; X<sub>3</sub>: SAA type, \*P<0.01 indicates significant difference

### Influence of formulation variables on vesicle size

Vesicle size is essential for transdermal delivery of drug-loaded nanocarriers and so submicron sizes permit an effective penetration into the stratum corneum [30]. As revealed in (table 2), the values for PDI and ZP ranged from 0.133±0.09 to 0.466±0.05 for the former and -19.00±1.50 mV to -27.5±1.75 mV for the latter. The vesicle size of all the prepared DKT-loaded TEs ranged from 50.36±3.03 nm to 133.2±1.62 nm where the formulation variables revealed a significant effect ( $p<0.0001$ ). For given levels of each variable, the coded equation yields an estimate of the response (Y<sub>2</sub>) where the coefficient of estimates for X<sub>1</sub> has a positive sign indicating a positive correlation between lipid S100 concentration and TE vesicle size which means that increasing the level of X<sub>1</sub> from 1% (89.97±2.11 nm) to 4% (133.2±1.62 nm) resulted in larger vesicle size. Phospholipid concentration (Lipoid S100) has been demonstrated to alter the vesicular size, with increasing phospholipid concentration increasing the vesicular size by continuing to increase bilayer width [33, 34]. On the contrary, X<sub>2</sub> and X<sub>3</sub> presented a negative correlation with VS based on the sign of the coefficient of estimates (-15.48 and -14.81). Altering the SAA concentration from 0.2% to 0.8% resulted in VS reduction from 93.51±1.78 nm to 51.61±2.50 nm. Since the amphiphilic head group occupies more space than the hydrophobic tail's cross-sectional area, the SAA molecule has a cone-like shape. When SAAs engage with lipid bilayers where the hydrophobic parts infiltrate the lipid bilayers and the polar head groups coupled to the lipid polar segments. Raising the SAA concentration widened the gap between both the hydrophobic chain lengths of Lipoid and SAA, prompting the curvature of lipid SAA aggregates to increase. As a result, the cone-shaped SAA disrupts the tightly packed lipid bilayers, resulting in reduced VS [35]. The data also revealed that the VS was proportional to the amount of drug entrapped in the vesicles. Thus, the %SE decrease would provide additional clarification for the lower VS [1]. In terms of SAA type (X<sub>3</sub>), the VS was higher for TEs formulae prepared employing cremophore than for corresponding formulations prepared containing Labrafil, which can be seen in (fig. 1). Yeo *et al.* [36] claimed that as the HLB value of SAA reduced, the VS increases, which is attributed to a reduction in the hydrophilic component of SAA. Therefore, labrafil with the low HLB value (9) compared to cremophore (HLB =15), as mentioned earlier, resulting in the highest VS. Abdulbaqi *et al.* [33] reported that TEs prepared *via* Labrafil revealed greater VS than that prepared using Tween 20 (HLB= 16.7).

The coded equation that clarified the influence of X<sub>1</sub>, X<sub>2</sub> and X<sub>3</sub> on VS is as follows:

$$Y_2 = 78.74 + 11.47 X_1 - 15.48 X_2 - 14.81 X_3$$

### Influence of formulation variables on release efficiency

The *in vitro* release profile of DKT from different prepared TEs can be seen in (fig. 2), confirming that all developed formulae

displayed controllable release within 8 h. As shown in (table 2), the values for %RE ranged from 44.62±1.36% to 82.98±2.60%, which is regarded as a controlled release compared to the DKT solution that recorded %RE of 86.57±0.16%. Statistical analysis demonstrated that all formulation variables possess a significant effect ( $p<0.0001$ ) on %RE where the most influence factor was X<sub>2</sub> (SAA concentration) (sum of squares = 1256.70) compared to X<sub>1</sub> (396.01) and X<sub>3</sub> (301.72). The impact of boosting Lipoid S100 concentration from 1% to 4% resulted in a decrease in %RE from 57.92±2.21% to 44.62±1.36%. This negative effect occurs due to the existence of compact and condensed vesicle structure at a high concentration which later delays DKT release [31]. Upon shifting the level of X<sub>2</sub> from low to high value, %RE increases from 44.62±1.36% to 66.39±1.24% which indicates a positive correlation between X<sub>2</sub> and X<sub>3</sub> (verified by the +sign of the coefficient of estimates). As stated previously, VS of TEs decreases with increased SAA concentration and hence increases surface area resulting in higher %RE [34]. A similar pattern also occurs in the case of X<sub>3</sub> where the vesicles prepared *via* labrafil attain %RE of 44.62±1.36% when compared to cremophore 56.72±2.38% and this is in harmony with the outcomes as per Albash *et al.* [1] where SAA with low HLB value slows down the drug release. This might be attributed to that TEs containing cremophore produce VS small compared to that prepared using labrafil, so resulted in increasing total surface area besides micelles [37] formation, which hence increases %RE [32].

The coded equation that clarified the influence of X<sub>1</sub>, X<sub>2</sub> and X<sub>3</sub> on %RE is as follows:

$$Y_3 = 65.00 - 4.97 X_1 + 8.86 X_2 + 4.34 X_3$$

### Optimization of the formulation through using the desirability function

For optimization, certain criteria were established for an assortment, including attaining the required VS, maximum % SE and lowest %RE as represented in (table 1) to fig. out the best formula with the relevant features. The optimal independent variable values were collected in the current study *via* numerical optimization according to acceptable criteria for all outcomes. The formula prepared utilizing a combination of 4% lipid S100 and 0.2% labrafil (F1) accomplished the mandatory criterion with a higher value of desirability (0.966) as illustrated in (fig. 1). Formerly, F1 was nominated to be subjected to further investigations where it was formulated as a gel using 1% w/w carbopol.

### Vesicles morphology of the optimized DKT loaded TEs gel using a Transmission electron microscope (TEM)

Fig. 3 displayed the morphological assessment of the optimum formula where uniform spherical-shaped vesicles were observed.

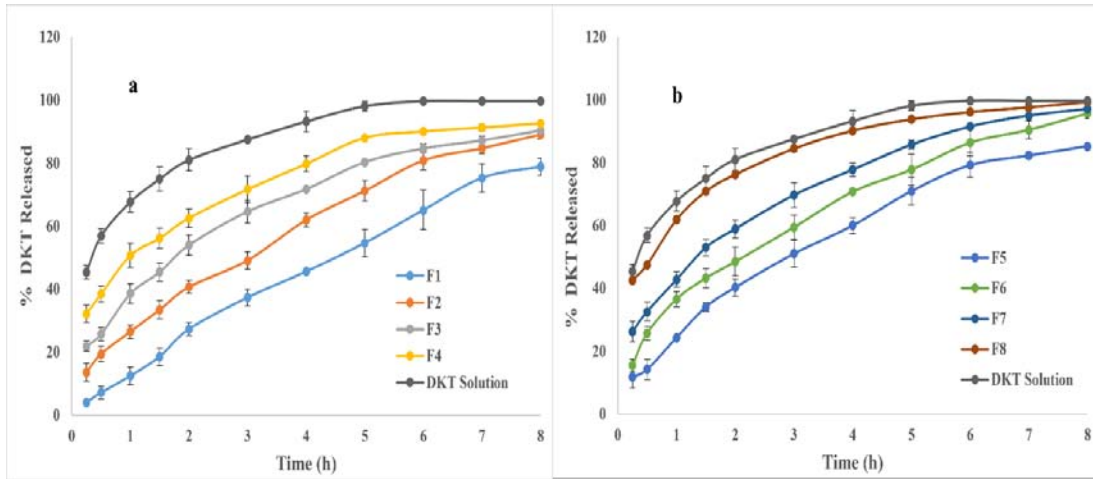


Fig. 2: *In vitro* release graphic illustration of DKT from TE (a): Labrafil; (b): Cremophor (results were expressed as mean±SD, n=3)

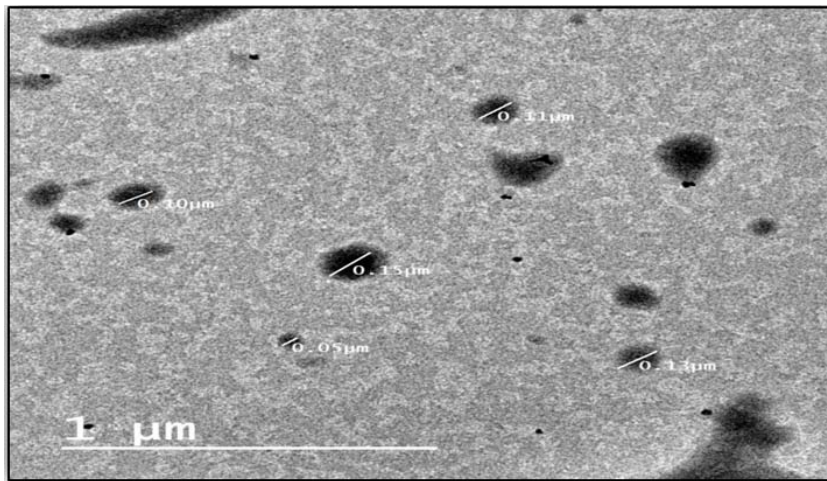


Fig. 3: TEM photomicrograph of the optimum TE formulation (F1)

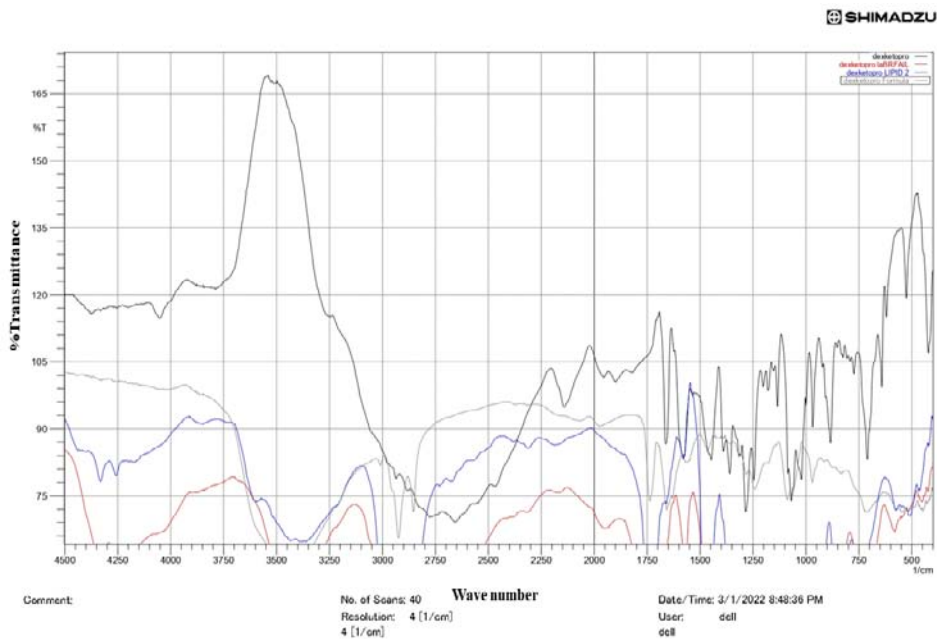


Fig. 4: FT-IR of DKT, TE components and optimum formulation (F1)

### Fourier transform infrared spectroscopy (FT-IR)

Fig. 4 displayed FT-IR spectra for DKT, lipid, labrafil, and optimum formula (F1). The characteristics peaks for DKT occur at  $1600\text{ cm}^{-1}$  and  $1650\text{ cm}^{-1}$  accredited to carbonyl vibrations; the benzopyran ring has alluded to  $860\text{ cm}^{-1}$  and  $690\text{ cm}^{-1}$ . Additionally, (fig. 4) displayed spectra for F1 where characteristic peaks were deprived of fluctuation, therefore indicating the absence of interaction between DKT and TE components [5].

### Ex-vivo skin permeation evaluation of DKT-loaded TEs gel

Fig. 5 displayed the outcomes for *ex vivo* skin permeation of DKT loaded TEs gel compared to DKT solution, where the results displayed a 2.6-fold increase in % DKT permeation upon comparing

the former with the latter as shown in (fig. 5). The inclusion of ethanol, phospholipids, and surfactants is accountable for the increased skin penetration considerably of DKT from TEs gels (F1) over DKT solution. These components strive to improve DKT skin penetration by enhancing the vesicle malleability and the skin lipid breakdown, resulting in a greater number of TEs infiltrating the skin's deepest layers and releasing the drug [26, 38].

### Stability study of the optimized DKT-loaded TE gel

Upon comparing the VS, PDI, ZP, %EE, and %RE of the optimized formula formerly and after storage, a non-significant change ( $P>0.05$ ) in all pre-mentioned assessments was observed, confirming that the optimized DKT loaded TE was stable under accelerated storage condition.

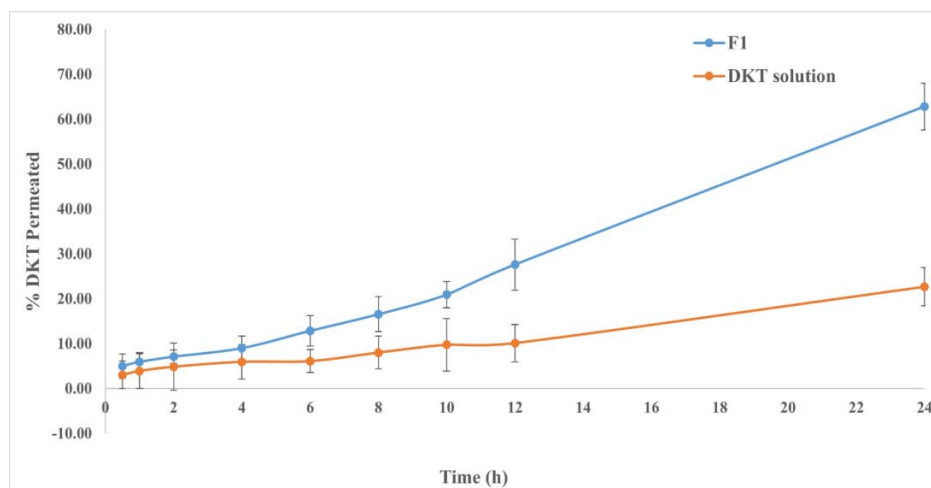


Fig. 5: *Ex-vivo* DKT permeation profile from the optimum TE formulation (F1) and DKT solution (results were expressed as mean $\pm$ SD, n=3)

### CONCLUSION

DKT-loaded TEs were formulated and optimized using full factorial design  $2^3$  as an experimental design to study the influence of different variables on TEs properties. The thin film hydration process was used to develop TEs where all prepared DKT-loaded TEs revealed acceptable VS, ZP and PDI. The optimized formula (F1) was selected based on achieving the highest %SE, acceptable VS, and lowest %RE, which was consequently renovated into gel to be ready for skin permeation. F1 revealed improved skin permeability better than DKT solution and it was stable under accelerated storage conditions. As a result, it is hypothesized that TEs gels are promising carriers for DKT transdermal administration. These carriers offer an alternative option for providing this therapy, bypassing the poor bioavailability and considerable adverse consequences of using the oral route. Finally, vesicular carriers have piqued the interest of experts in the domain of innovative drug delivery, maintaining the relevance of vesicular carrier applications in therapeutics and pharmaceutical delivery.

### FUNDING

Nil

### AUTHORS CONTRIBUTIONS

All the authors have contributed equally.

### CONFLICT OF INTERESTS

No conflict of interest was declared by the authors

### REFERENCES

- Albasha R, Abdelbary AA, Refai H, El-Nabarawi MA. Use of transethosomes for enhancing the transdermal delivery of olmesartan medoxomil: *in vitro*, *ex vivo*, and *in vivo* evaluation. *Int J Nanomedicine*. 2019;14:1953-68. doi: 10.2147/IJN.S196771, PMID 30936696.
- Sivaraman A, Banga AK. Novel in situ forming hydrogel microneedles for transdermal drug delivery. *Drug Deliv Transl Res*. 2017;7(1):16-26. doi: 10.1007/s13346-016-0328-5, PMID 27562294.
- Song H, Wen J, Li H, Meng Y, Zhang Y, Zhang N. Enhanced transdermal permeability and drug deposition of rheumatoid arthritis via sinomenine hydrochloride-loaded antioxidant surface transethosome. *Int J Nanomedicine*. 2019;14:3177-88. doi: 10.2147/IJN.S188842, PMID 31118630.
- Song CK, Balakrishnan P, Shim CK, Chung SJ, Chong S, Kim DD. A novel vesicular carrier, transethosome, for enhanced skin delivery of voriconazole: characterization and *in vitro/in vivo* evaluation. *Colloids Surf B Biointerfaces*. 2012;92:299-304. doi: 10.1016/j.colsurfb.2011.12.004, PMID 22205066.
- Öztürk AA, Kıyan HT. Treatment of oxidative stress-induced pain and inflammation with dexamethasone loaded different molecular weight chitosan nanoparticles: formulation, characterization and anti-inflammatory activity by using *in vivo* HET-CAM assay. *Microvasc Res*. 2020;128:103961. doi: 10.1016/j.mvr.2019.103961, PMID 31758946.
- Meng S, Chen Z, Yang L, Zhang W, Liu D, Guo J. Enhanced transdermal bioavailability of testosterone propionate via surfactant-modified ethosomes. *Int J Nanomedicine*. 2013;8:3051-60. doi: 10.2147/IJN.S46748, PMID 23990718.
- Chen ZX, Li B, Liu T, Wang X, Zhu Y, Wang L. Evaluation of paeonol-loaded transethosomes as transdermal delivery carriers. *Eur J Pharm Sci*. 2017;99:240-5. doi: 10.1016/j.ejps.2016.12.026, PMID 28039091.
- Azizah N, Sagita E, Iskandarsyah I. *In vitro* penetration tests of transethosome gel preparations containing capsaicin. *Int J App Pharm*. 2017;9:116. doi: 10.22159/ijap.2017.v9s1.68\_75.
- Mishra KK. Withdrawal notice: development of itraconazole-loaded transethosomes for improved transdermal delivery. *Recent Pat Nanotechnol*. 2021. doi: 10.2174/1872210515666211129115811, PMID 34844550.

10. Al Shuwaili AH, Rasool BK, Abdulrasool AA. Optimization of elastic transfersomes formulations for transdermal delivery of pentoxifylline. *Eur J Pharm Biopharm.* 2016;102:101-14. doi: 10.1016/j.ejpb.2016.02.013, PMID 26925505.
11. Ma M, Wang J, Guo F, Lei M, Tan F, Li N. Development of nanovesicular systems for dermal imiquimod delivery: physicochemical characterization and *in vitro/in vivo* evaluation. *J Mater Sci Mater Med.* 2015;26(6):191. doi: 10.1007/s10856-015-5524-1, PMID 25989936.
12. Castillo Henriquez L, Sanabria Espinoza P, Murillo Castillo B, Montes de Oca-Vasquez G, Batista Menezes D, Calvo Guzman B. Topical chitosan-based thermo-responsive scaffold provides dexketoprofen trometamol controlled release for 24 h use. *Pharmaceutics.* 2021;13(12). doi: 10.3390/pharmaceutics13122100, PMID 34959381.
13. Ferrara F, Benedusi M, Sguizzato M, Cortesi R, Baldisserotto A, Buzzi R. Ethosomes and transthesosomes as cutaneous delivery systems for quercetin: A preliminary study on melanoma cells. *Pharmaceutics.* 2022;14(5). doi: 10.3390/pharmaceutics14051038.
14. Rodriguez Luna A, Talero E, Avila Roman J, Romero AMF, Rabasco AM, Motilva V. Preparation and *in vivo* evaluation of rosmarinic acid-loaded transthesosomes after percutaneous application on a psoriasis animal model. *AAPS PharmSciTech.* 2021;22(3):103. doi: 10.1208/s12249-021-01966-3, PMID 33712964.
15. Chen M, Liu X, Fahr A. Skin penetration and deposition of carboxyfluorescein and temoporfin from different lipid vesicular systems: *in vitro* study with finite and infinite dosage application. *Int J Pharm.* 2011;408(1-2):223-34. doi: 10.1016/j.ijpharm.2011.02.006, PMID 21316430.
16. Abd El-Halim SM, Abdelbary GA, Amin MM, Zakaria MY, Shamsel-Din HA, Ibrahim AB. Stabilized oral nanostructured lipid carriers of adefovir dipivoxil as a potential liver targeting: estimation of liver function panel and uptake following intravenous injection of radioiodinated indicator. *Daru.* 2020;28(2):517-32. doi: 10.1007/s40199-020-00355-8, PMID 32564282.
17. Das S, Chaudhury A. Recent advances in lipid nanoparticle formulations with solid matrix for oral drug delivery. *AAPS PharmSciTech.* 2011;12(1):62-76. doi: 10.1208/s12249-010-9563-0, PMID 21174180.
18. Verma S, Bhardwaj A, Vij M, Bajpai P, Goutam N, Kumar L. Oleic acid vesicles: a new approach for topical delivery of antifungal agent. *Artif Cells Nanomed Biotechnol.* 2014;42(2):95-101. doi: 10.3109/21691401.2013.794351, PMID 23656670.
19. Sudhakar K, Mishra V, Jain S, Rompicherla NC, Malviya N, Tambuwala MM. Development and evaluation of the effect of ethanol and surfactant in vesicular carriers on lamivudine permeation through the skin. *Int J Pharm.* 2021;610:121226. doi: 10.1016/j.ijpharm.2021.121226, PMID 34710540.
20. Farooq M, Usman F, Zaib S, Shah HS, Jamil QA, Akbar Sheikh F. Fabrication and evaluation of voriconazole loaded Transthesosomal gel for enhanced antifungal and antileishmanial activity. *Molecules.* 2022;27(10). doi: 10.3390/molecules27103347, PMID 35630825.
21. Garg V, Singh H, Bhatia A, Raza K, Singh SK, Singh B. Systematic development of Transthesosomal gel system of piroxicam: formulation optimization, *in vitro* evaluation, and ex vivo assessment. *AAPS PharmSciTech.* 2017;18(1):58-71. doi: 10.1208/s12249-016-0489-z, PMID 26868380.
22. Abdellatif MM, Khalil IA, Khalil MAF. Sertaconazole nitrate loaded nanovesicular systems for targeting skin fungal infection: *in vitro*, ex-vivo and *in vivo* evaluation. *Int J Pharm.* 2017;527(1-2):1-11. doi: 10.1016/j.ijpharm.2017.05.029, PMID 28522423.
23. ElMeshad AN, Abdel Haleem KM, Abdel Gawad NA, El-Nabarawi MA, Sheta NM. Core in cup ethylmorphine hydrochloride tablet for dual fast and sustained pain relief: formulation, characterization, and pharmacokinetic study. *AAPS PharmSciTech.* 2020;21(7):244. doi: 10.1208/s12249-020-01759-0, PMID 32856114.
24. Sheta NM, Boshra SA, Mamdouh MA, Abdel-Haleem KM. Design and optimization of silymarin loaded in lyophilized fast melt tablets to attenuate lung toxicity induced via HgCl<sub>2</sub> in rats. *Drug Deliv.* 2022;29(1):1299-311. doi: 10.1080/10717544.2022.2068696, PMID 35470762.
25. Teaima HM, Abdel Haleem KM, Osama M, El-Nabarawi MA, M Fayed S. Bi-laminated oral disintegrating film for dual delivery of pitavastatin calcium and lornoxicam: fabrication, characterization and pharmacokinetic study. *Int J App Pharm.* 2022;14(2):53-60.
26. Ascenso A, Raposo S, Batista C, Cardoso P, Mendes T, Praça FG. Development, characterization, and skin delivery studies of related ultra deformable vesicles: transfersomes, ethosomes, and transthesosomes. *Int J Nanomedicine.* 2015;10:5837-51. doi: 10.2147/IJN.S86186, PMID 26425085.
27. Mendes AC, Gorzelanny C, Halter N, Schneider SW, Chronakis IS. Hybrid electrospun chitosan-phospholipids nanofibers for transdermal drug delivery. *Int J Pharm.* 2016;510(1):48-56. doi: 10.1016/j.ijpharm.2016.06.016, PMID 27286632.
28. Moolakkadath T, Aqil M, Ahad A, Imam SS, Iqbal B, Sultana Y. Development of transthesosomes formulation for dermal fisetin delivery: Box-Behnken design, optimization, *in vitro* skin penetration, vesicles-skin interaction and dermatokinetic studies. *Artif Cells Nanomed Biotechnol.* 2018;46(Suppl):755-65. doi: 10.1080/21691401.2018.1469025, PMID 29730964.
29. Shah H, Nair AB, Shah J, Bharadia P, Al-Dhubiab BE. Proniosomal gel for transdermal delivery of lornoxicam: optimization using factorial design and *in vivo* evaluation in rats. *Daru.* 2019;27(1):59-70. doi: 10.1007/s40199-019-00242-x, PMID 30701460.
30. Teaima M, Abdelmonem R, Adel YA, El-Nabarawi MA, El-Nawawy TM. Transdermal delivery of telmisartan: formulation, *in vitro*, ex vivo, iontophoretic permeation enhancement and comparative pharmacokinetic study in rats. *Drug Des Devel Ther.* 2021;15:4603-14. doi: 10.2147/DDDT.S327860, PMID 34785889.
31. Aboud HM, Ali AA, El-Menshawe SF, Elbary AA. Nanotransfersomes of carvedilol for intranasal delivery: formulation, characterization and *in vivo* evaluation. *Drug Deliv.* 2016;23(7):2471-81. doi: 10.3109/10717544.2015.1013587, PMID 25715807.
32. Al-Mahallawi AM, Abdelbary AA, Aburahma MH. Investigating the potential of employing bilosomes as a novel vesicular carrier for transdermal delivery of tenoxicam. *Int J Pharm.* 2015;485(1-2):329-40. doi: 10.1016/j.ijpharm.2015.03.033, PMID 25796122.
33. Abdulbaqi IM, Darwis Y, Assi RA, Khan NAK. Transthesosomal gels as carriers for the transdermal delivery of colchicine: statistical optimization, characterization, and ex vivo evaluation. *Drug Des Devel Ther.* 2018;12:795-813. doi: 10.2147/DDDT.S158018, PMID 29670336.
34. Alhakamy NA, Aldawsari HM, Ali J, Gupta DK, Warsi MH, Bilgrami AL. Brucine-loaded transliposomes nanogel for topical delivery in skin cancer: statistical optimization, *in vitro* and dermatokinetic evaluation. *3 Biotech.* 2021;11(6):288. doi: 10.1007/s13205-021-02841-5, PMID 34109091.
35. Chen Y, Qiao F, Fan Y, Han Y, Wang Y. Interactions of cationic/anionic mixed surfactant aggregates with phospholipid vesicles and their skin penetration ability. *Langmuir.* 2017;33(11):2760-9. doi: 10.1021/acs.langmuir.6b04093, PMID 28013540.
36. Yeo LK, Olusanya TOB, Chaw CS, Elkordy AA. Brief effect of a small hydrophobic drug (cinnarizine) on the physicochemical characterisation of niosomes produced by thin-film hydration and microfluidic methods. *Pharmaceutics.* 2018;10(4). doi: 10.3390/pharmaceutics10040185, PMID 30322124.
37. Miyazawa T, Itaya M, Burdeos GC, Nakagawa K, Miyazawa T. A critical review of the use of surfactant-coated nanoparticles in nanomedicine and food nanotechnology. *Int J Nanomedicine.* 2021;16:3937-99. doi: 10.2147/IJN.S298606, PMID 34140768.
38. Bragagni M, Mennini N, Maestrelli F, Cirri M, Mura P. Comparative study of liposomes, transfersomes and ethosomes as carriers for improving topical delivery of celecoxib. *Drug Deliv.* 2012;19(7):354-61. doi: 10.3109/10717544.2012.724472, PMID 23043648.